Colour polymorphism associated with a gene duplication in male wood tiger moths

Melanie N. Brien[1*†], Anna Orteu[2*], Eugenie C. Yen[2], Juan A. Galarza[1,3], Jimi Kirvesoja[3], Hannu Pakkanen[4], Kazumasa Wakamatsu[5], Chris D. Jiggins[2**], Johanna Mappes[1,3**].

[1]*Organismal and Evolutionary Biology Research Program, Faculty of Biological and Environmental Sciences, University of Helsinki, Finland.*

[2]*Department of Zoology, University of Cambridge, United Kingdom.*

[3]*Department of Biological and Environmental Science, University of Jyväskylä, Finland.*

[4]*Department of Chemistry, University of Jyväskylä, Finland.*

[5]*Institue for Melanin Chemistry, Fujita Health University, Toyoake, Japan.*

*These authors contributed equally.

**Co-senior authors.

†Correspondence: mnbrien1@gmail.com

Abstract

Colour is often used as an aposematic warning signal, with predator learning expected to lead to a single colour pattern within a population. However, there are many puzzling cases where aposematic signals are also polymorphic. The wood tiger moth, *Arctia plantaginis*, uses bright hindwing colours as a signal of unpalatability, and males have discrete colour morphs which vary in frequency geographically. In Finland, both white and yellow morphs can be found, and these colour morphs also differ in behavioural and life-history traits. Complex polymorphisms such as these are often explained by supergenes. Here, we show that male colour is linked to an extra copy of a *yellow* family gene that is only present in the white morphs. This white-specific duplication, which we name *valkea,* is highly upregulated during wing development, and could act to reduce recombination, thus potentially representing a supergene. We also characterise the pigments responsible for yellow, white and black colouration, showing that yellow is partly produced by pheomelanins, while black is dopamine-derived eumelanin. The *yellow* family genes have been linked to melanin synthesis and behavioural traits in other insect species. Our results add to only a few examples of seemingly paradoxical and complex polymorphisms which are associated with single genes.

Introduction

Colour polymorphisms, defined as the presence of multiple discrete colour phenotypes within a population (Huxley, 1955), provide an ideal trait to study natural and sexual selection. Colour phenotypes are linked to fitness in many contexts including camouflage, mimicry and mating success. Colour is often associated with aposematism, warning predators of unpalatability (Cott, 1940; Cuthill *et al.*, 2017), and in such cases, predator learning should favour the most common colour pattern, leading to positive frequency dependent selection (Endler, 1988). Despite this, aposematic polymorphisms can be stable when selection is context-dependent (Briolat *et al.*, 2019), especially where genetic correlations between colour phenotypes and other traits lead to complex fitness landscapes (reviewed by McKinnon and Pierotti, 2010).

A variety of genetic mechanisms can underpin these types of complex polymorphisms involving multiple associated traits (Orteu and Jiggins, 2020). In many cases, such complex polymorphisms are controlled by 'supergenes' in which divergent alleles at several linked genes are maintained in strong linkage disequilibrium by reduced recombination. The most common mechanism for locally reduced recombination are inversions, which range from single inversions involving a small number of genes, to multiple nested inversions covering large genomic regions (Wang *et al.*, 2013; Küpper *et al.*, 2016; Tuttle *et al.*, 2016). Nonetheless, other mechanisms for reducing recombination, such as centromeres or large genomic deletions, may also play a role. An alternative mechanism is that a single regulatory gene could act in the same way as a supergene, by controlling variation via multiple downstream effects (Thompson and Jiggins, 2014). While there are fewer instances in which multiple phenotypes seem to be controlled by a single gene, one potential example is the common wall lizard, where colour genes have pleiotropic effects on behavioural and reproductive traits (Andrade *et al.*, 2019). Multiple mutations within a single gene can also lead to variation in multiple traits (Linnen *et al.*, 2013).

The wood tiger moth, *Arctia plantaginis,* has a complex polymorphism that has been well studied in an ecological context. Males show polymorphic aposematic hindwing colouration with discrete yellow, white or red hindwing colour morphs found at varying frequencies in different geographic locations. In Finland, for example, both yellow and white morphs can be found, with white morphs varying in frequency from 40 to 75% (Galarza *et al.*, 2014). In Estonia, white morphs make up 97% of the population, while yellows morphs form a

completely monomorphic population in Scotland (Hegna, Galarza and Mappes, 2015) (Figure 1). Long term breeding studies of these moths have shown that male hindwing colour is a Mendelian trait controlled by a single locus with two alleles (Suomalainen, 1938; Nokelainen *et al.*, 2022). White alleles (W) are dominant over the yellow (y). These colour genotypes also covary with behavioural and life-history traits, contributing to the maintenance of this polymorphism. Yellow males are subject to lower levels of predation in the wild (Nokelainen *et al.*, 2012, 2014), while white males have a positive frequency-dependent mating advantage (Gordon *et al.*, 2015). Yellow morphs have stronger chemical defences (Rojas *et al.*, 2017), but show reduced flight activity compared to white males, although yellows may fly at more selective times, i.e. at peak female calling periods (Rojas, Gordon and Mappes, 2015). In summary, there is a trade-off between natural selection through predation and reproductive success, which contributes to the maintenance of this polymorphism (Rönkä *et al.*, 2020).

Despite the large body of research on *A. plantaginis* colour morphs, the genetic basis of this polymorphism is unknown. Here, we explore the genetic basis of male hindwing colour using wild populations and lab crosses to test whether the polymorphism is associated with large structural rearrangements controlling multiple phenotypic elements, or the result of a single gene mutation. We then narrow down the candidate genes using a differential gene expression analysis and identify the pigments producing yellow, white and black colouration on the wings of male *A. plantaginis*.

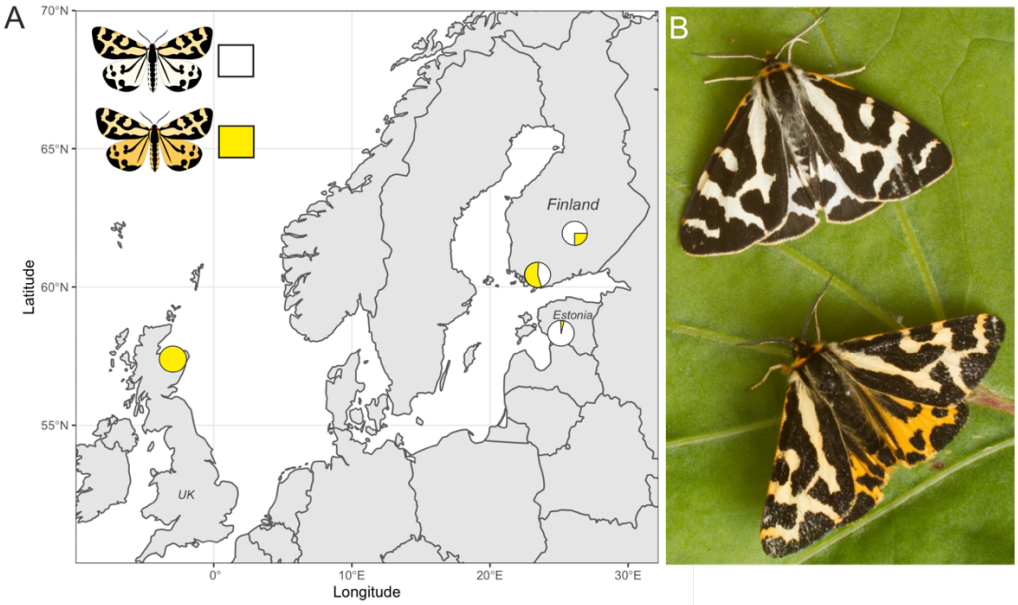

Figure 1: (A) Sampling locations and frequencies of yellow and white *Arctia plantaginis* in Finland, Scotland and Estonia. (B) Males of the white and yellow colour morphs (Credit: Samuel Waldron).

86 **Results**

87 *A narrow genomic region is associated with hindwing colour*

88 To investigate the genetic basis of male hindwing colouration in *A. plantaginis*, we carried
89 out a quantitative trait locus (QTL) mapping analysis using crosses between heterozygous
90 Wy males and homozygous yy females. We used RADseq data aligned to the yellow *A.*
91 *plantaginis* reference genome from 172 male offspring (90 white and 82 yellow) from four
92 families. The QTL analysis identified a single marker associated with male hindwing colour
93 (Figure 2). This marker was found on scaffold YY_tarseq_206_arrow at position 9,887,968bp
94 (95% confidence intervals 9,349,978-9,888,009bp) and had a LOD score of 32.8 ($p<0.001$).
95 The significant marker explains around 75% of the phenotypic variation and, with one
96 exception, yellow individuals all had a homozygous yy genotype at this marker. This is
97 consistent with tight linkage of this marker to the causal SNP.

98 To further narrow down this region, we ran a genome wide association study (GWAS) using
99 whole genome sequences of males from four populations: Southern Finland (5 white, 5
100 yellow) and Central Finland (10 w, 10 y), where male morphs are either white or yellow,
101 Estonia (4 w), where males are mostly white, and Scotland (12 y), where all males are
102 yellow. This identified a region of associated SNPs also on scaffold 206 (Figure 2). Two
103 SNPs, 137bp apart (at positions 9,885,384 and 9,885,521), were significant above a strict
104 Bonferroni corrected threshold. 162 SNPs were over the threshold of $p<0.0001$ and, of these,
105 155 are within a 99kb region on scaffold 206 (9,833,387-9,932,264bp). The top SNPs are
106 within 2.5kb from the top QTL marker, and the SNP at this marker has a p-value <0.0001.

107 The 538Kb QTL interval contains 21 genes (Table S1) which were annotated with reference
108 to *D. melanogaster*. Of these genes, four are part of the *yellow* gene family. The top two
109 SNPs from the GWAS, and the top marker from the QTL, fall in a non-coding region
110 upstream of the gene, *yellow-e*, and are also close to an additional *yellow* gene, *yellow-g.*

111 *Identifying structural variation in this region*

112 The trio binning method used by Yen et al. (2020) to assemble the *A. plantaginis* reference
113 genome produced two reference sequences, one for a white allele and one for a yellow allele.
114 We extracted the region containing the QTL interval from the yellow reference and aligned it
115 against the white reference. The alignment showed a duplicated region approximately 117kb

116 long on scaffold 419 of the white reference from around 6,941,000-7,058,000bp (Figure S1).
117 The *yellow-e* gene and its flanking regions are within this sequence and are therefore
118 duplicated in the white reference (Figure 2). One copy of the gene (named jg1310 in the W
119 annotation) has 7 exons and is similar to the *yellow-e* gene in the yellow reference (99.7%
120 identity in coding sequences). The second copy unique to the white scaffold (jg1308) has
121 only the first 5 exons (81.8% identical to the gene in the yellow reference), possibly due to a
122 stop codon mutation in the 5th exon. For clarity, we named this duplicated white-specific
123 copy *valkea*, in reference to a Finnish term for 'white'. While all white samples had
124 consistent coverage of reads across the duplicated region, coverage was patchy in yellow
125 samples, with many regions having no coverage in yellow samples (Figure 2). Those reads
126 that map in the *valkea* region in yellow samples are likely to be mapping errors.
127
128 To confirm that both of these gene copies are related to *yellow-e*, we compared them to
129 *yellow-e* orthologs found in *Bombyx mori*, *Heliconius melpomene* and *Drosophila*
130 *melanogaster,* along with other *yellow* genes from *A. plantaginis* and *B. mori*. Both of the
131 tiger moth genes were most closely related to the *H. melpomene yellow-e* (Figure S2).
132 Between *valkea* and *yellow-e* there is an additional gene which showed highest similarity to
133 *Drosophila yellow-g2* (when extracted from both the white and yellow references). This gene
134 is not part of the duplicated sequence and is present as a single copy in both morphs.
135 Coverage across *yellow-g* and *yellow-e* genome regions in wild samples is similar in both
136 morphs (Figure 2).
137

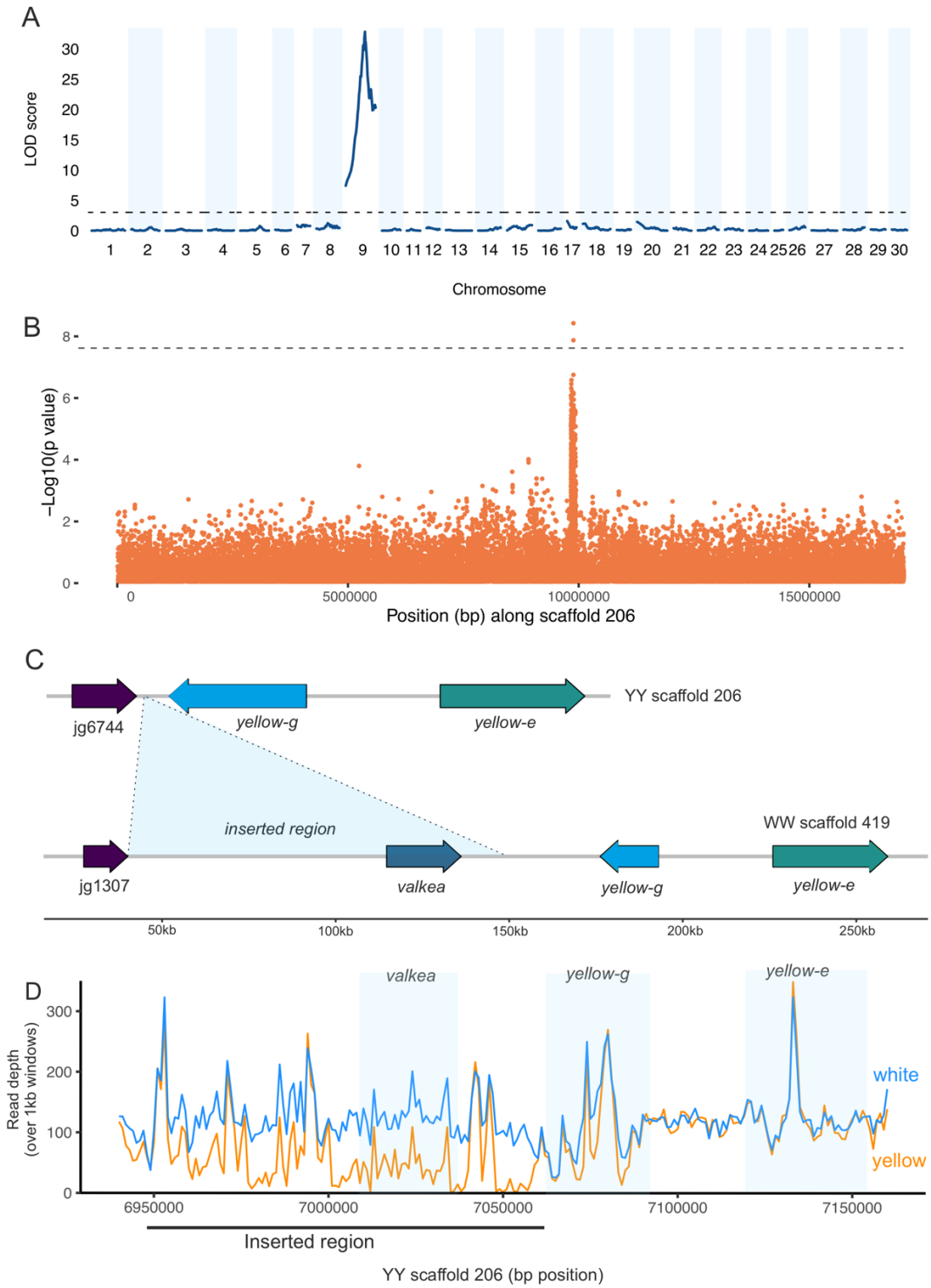

Figure 2: (A) QTL analysis reveals a 500kb region significant on scaffold 206, part of linkage group 9. (B) A GWAS of wild samples showed SNPs associated with hindwing colour along the same scaffold. The dotted line shows the Bonferroni corrected significance threshold. (C) An insertion in the white reference sequence contains a copy of the *yellow-e* gene, which we named *valkea*, in addition to the *yellow-e* present in both white and yellow morphs. (D) Read depth across the candidate region in all Finnish white and yellow samples.

145 *Valkea is differentially expressed between morphs*

146 To pinpoint which of these candidate genes is associated with male wing polymorphism in *A.*
147 *plantaginis,* we next performed gene expression analyses across several developmental
148 stages. Based on knowledge of the expression patterns of *yellow* genes and other colour
149 pattern genes such as *optix* (Reed *et al.*, 2011) and *cortex* (Nadeau *et al.*, 2016) in
150 Lepidoptera, we hypothesised that changes in gene regulation that control the development of
151 wing colour morphs in the tiger moth most likely occur during pupal development. Pupal
152 development in the wood tiger moth lasts for approximately 8 days, and no colour is present
153 in the wings until day 7, when the yellow pigment appears. A few hours later, black melanin
154 pigmentation is deposited. We sampled two stages early in development when no colouration
155 is present in the wings (72 hours post-pupation, and 5 day old pupae), and two stages later in
156 development: the point when yellow appears in yy morphs (Pre-mel, 7 day old pupae) and the
157 other after black melanin has also been deposited (Mel, 7-8 days old). Five individuals per
158 genotype and stage were sampled.

159 We analysed differential gene expression using the W reference genome, which contains the
160 duplicated region that includes *valkea*. Developmental stage was the main factor explaining
161 most of the genome-wide variation in gene expression between samples (Figure S3). Such a
162 pattern would be expected as many genes are involved in development and thus are likely to
163 be differentially expressed (DE) between developmental stages. No apparent clustering can
164 be observed among samples of the same colour morph.

165 We next compared gene expression between yy and WW individuals at each of the
166 developmental stages. From the 22 genes identified in the GWAS and QTL analysis, only
167 two, *yellow-e* and *valkea*, were differentially expressed in any of the comparisons. *Valkea*
168 was overexpressed in white individuals in the pre-melanin stage with a Log Fold Change of
169 10.32 and a p-value of 2.18e-06. As *valkea* is only fully present in the W genome, it is not
170 expected to be expressed at all in the Y genome. *Yellow-e* was also overexpressed in white
171 individuals with a Log Fold Change of 3.86 and adjusted p-value of 5.62e-06. In other
172 developmental stages, neither *valkea* nor *yellow-e* showed differences in expression between
173 morphs (Figure 3).

174 The GWAS and QTL peaks of association are situated in scaffold 419 of the WW reference
175 assembly, which in a WW linkage map forms a linkage group along with 6 more scaffolds

176 (472, 487, 515, 531, 540 and 609). We found that 12 genes present in this linkage group were
177 differentially expressed, including *valkea* and *yellow-e* (Table S2), and identified their
178 orthologues in *Drosophila melanogaster*.

179 We next conducted a genome-wide analysis of the RNA-seq data. Lowly expressed genes
180 were filtered out with 10,920 genes retained. Overall, 99 genes were differentially expressed
181 (FDR < 0.05) between the two morphs. Of these, 49 were upregulated in the yy morph, while
182 the remaining 50 were upregulated in WW individuals. The earliest developmental stage, 72-
183 hours, was the stage with the highest number of DE genes (n = 48), while the 5-day old stage
184 had the fewest (n=7). One gene which encodes a C2H2 zinc finger transcription factor in *D.*
185 *melanogaster*, *'jg15945',* was over-expressed in yy in the first three stages (Figure S4).

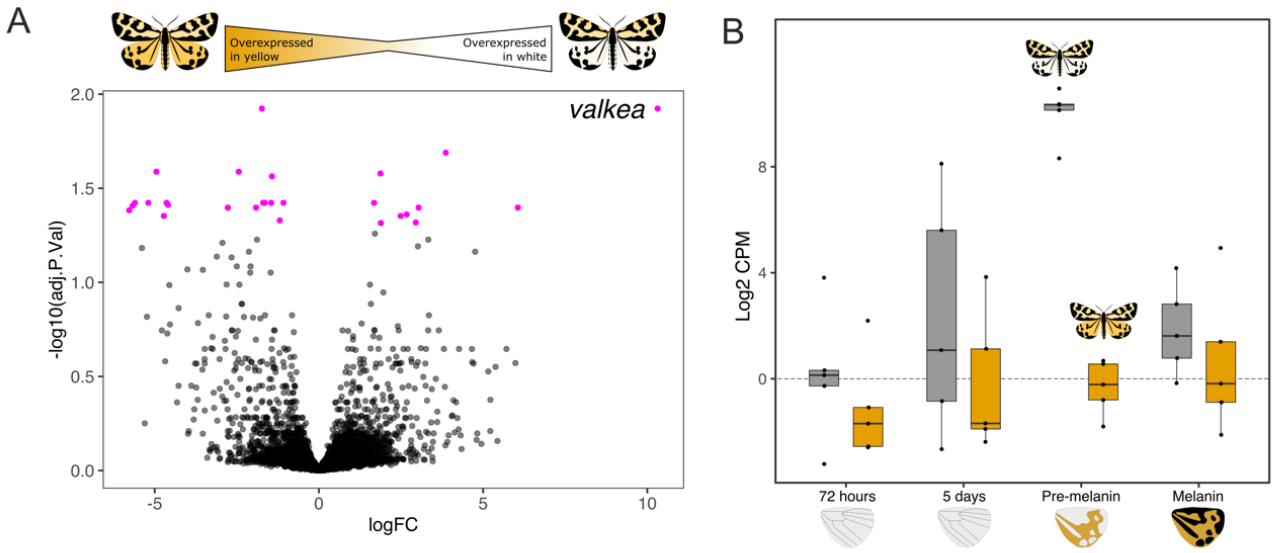

186

187 Figure 3: (A) RNA-seq of developing wings shows 99 genes that are differentially expressed between
188 morphs. (B) *Valkea* is highly expressed in the white morph at the pre-melanin stage. Expression of
189 *valkea* in yellow morphs is around 0.

190 *Yellow-e is not associated with colour*

191 We next used a tree topology approach to explore the relationships between alleles around the
192 duplicated sites among the populations. For four populations (Finnish white and yellow,
193 Estonian and Scottish populations), three topologies are possible; grouping populations by
194 colour, by geography and one grouping neither by colour nor geography. At *yellow-e*, the
195 highest weighting is towards the geography grouping, suggesting that this gene is not
196 associated with the colour switch (Figure S5).

197

198 *Pigment analysis*

199 Since the *yellow* gene family, to which *valkea* is related, is known to be responsible for the
200 production of melanin pigments, we further investigated the identity of the wing
201 pigmentation. First, we ruled out the presence of several non-melanin pigment types in the
202 hindwings, including pterins and carotenoids. Pterins are commonly found in insects and,
203 along with purine derivatives, papiliochromes and flavonoids, are soluble in strong acids and
204 bases or in organic solvents (Umebachi, 1975; Kayser, 1985; Shamim *et al.*, 2014). We
205 placed wing samples from each morph in NaOH overnight, then measured the absorbance of
206 the supernatant using a spectrophotometer. We also left wings in methanol overnight before
207 measuring the supernatant. The spectra did not show any peaks indicative of any pigment
208 dissolved in the sample. Similarly, we found no evidence for carotenoid pigments after
209 dissolving in a hexane:tert-butyl methyl ether solution (Figure S6). Wings did not fluoresce
210 under UV light, providing further evidence for the lack of fluorescent pigments including
211 pterins, flavonoids, flavins and papiliochromes (Umebachi, 1975; Kayser, 1985).
212 Ommochromes are red and yellow pigments; high performance liquid chromatography
213 (HPLC) ruled out the presence of these pigments on the moth wings, which we compared to
214 data from ommochrome-containing *Heliconius* wings and a Xanthurenic acid standard
215 (Figure S7).

216 HPLC analysis showed peaks characteristic of pheomelanin (Figure S8). Pheomelanins
217 produce red-brown colour in grasshoppers and wasps (Galván *et al.*, 2015; Jorge García,
218 Polidori and Nieves-Aldrey, 2016), and orange-red colours in ants and bumblebees (Hines *et*
219 *al.*, 2017; Polidori, Jorge and Ornosa, 2017). Insects generally have dopamine-derived
220 pheomelanin and a breakdown product of this is 4-Amino-3-hydroxyphenylethylamine (4-
221 AHPEA) (Barek *et al.*, 2018). Yellow wings showed large peaks for 4-AHPEA. White wings
222 had around 27% of the 4-AHPEA levels seen in yellow wings, and black sections of the
223 wings had 16%. Hydrogen iodide hydrolysis of wings produced the isomer 3-AHPEA, which
224 may come from 3-nitrotyramine originating from the decarboxylation of 3-nitrotyrosine.
225 Reduction of 3-nitrotyrosine produces 3-AHP, another marker of pheomelanin (Wakamatsu,
226 Ito and Rees, 2002).
227
228 Analysis of the black portions of the wing found pyrrole-2,3-dicarboxylic acid (PDCA) and
229 pyrrole-2,3,5-tricarboxylic acid (PTCA) (Figure S9). Both are components of eumelanin

230 (Barek *et al.*, 2018), suggesting that the black colouration seen in the wood tiger moth is
231 predominantly eumelanin derived from dopamine. This is common in producing black
232 colouration and providing structural components of the exoskeleton. In addition, dopamine is
233 acylated to both *N*-β-alanyldopamine (NBAD) and *N*-acetyldopamine (NADA) sclerotins.
234 NADA sclerotins are colourless and likely to be present on the white wings. This analysis of
235 pigmentation is therefore consistent with a role for *yellow* family genes in regulating the
236 colour polymorphism.

237 **Discussion**

238 Hindwing colouration of male *Arctia plantaginis* is polymorphic and these colour morphs
239 vary in multiple behavioural and life-history traits, providing an example of a complex
240 polymorphism. Here, we have shown that variation in male hindwing colour is associated
241 with a narrow region in the genome, characterised by a duplicated sequence found only in
242 white morphs and containing a gene from the *yellow* gene family. The white-specific copy,
243 *valkea,* is highly expressed during pupal development, consistent with genetic dominance of
244 the white allele. The presence of only one gene is in contrast to 'classical' supergenes which
245 often explain the genetic architecture of complex polymorphisms (Thompson and Jiggins,
246 2014) and involve chromosomal rearrangements containing multiple genes that allow the
247 maintenance of co-adapted haplotypes (Joron *et al.*, 2006; Lowry and Willis, 2010; Küpper *et*
248 *al.*, 2016; Funk *et al.*, 2021).

249 Although we did not find evidence for a supergene involving multiple loci, this morph-
250 specific duplication still provides a region of reduced recombination between morphs. This is
251 similar to the genetic architecture of the *Primula* supergene controlling heterostyly, which
252 involves a large duplication containing five genes (Huu *et al.*, 2020). The duplicated region is
253 effectively hemizygous and cannot recombine except in homozygote genotypes, which could
254 contribute to the maintenance of the complex polymorphism and the linkage of multiple
255 traits. In polymorphic *Papilio dardanus*, one colour pattern morph is associated with a
256 duplicated region, again providing physical constraints on recombination (Timmermans *et*
257 *al.*, 2014). Nonetheless, in the case of the wood tiger moth, it remains unclear how a single
258 gene, such as *valkea*, can control the development of a broad array of phenotypic traits.

259 One possible mechanism is that there is a regulatory element along the scaffold which is
260 controlling colour via the *valkea* gene, but also regulating other genes to control different

261 phenotypic traits. We found the most significant markers and SNPs located in a non-coding
262 region close to the *yellow* genes, which likely contains a cis-regulatory element (CRE)
263 controlling transcription of *valkea.* In cichlids, for example, a CRE at the gene encoding
264 agouti-related peptide 2 controls variation in strip patterning in two closely related species
265 (Kratochwil *et al.*, 2018).

266 Differential expression of other genes on the same chromosome controlled by the CRE could
267 explain variation in covarying traits. The over-expression of another gene, possibly encoding
268 a zinc transcription factor, in yellow individuals in the early pupal stages suggests that there
269 is differential expression of unlinked genes as a result of the polymorphism, although since
270 this gene is on a different chromosome to *valkea* it is unlikely to be directly controlled by the
271 CRE. Another hypothesis is that somehow *valkea* itself regulates other genes. However,
272 *yellow* family genes are not known to regulate transcription of other genes, unlike for
273 example *doublesex*, a transcription factor that undergoes alternative splicing and female
274 mimetic wing pattern polymorphism in *Papilio polytes* (Kunte *et al.*, 2014; Nishikawa *et al.*,
275 2015).

276 The *yellow* family genes are highly conserved throughout insects (Ferguson *et al.*, 2011).
277 They have been widely linked to colouration (Wittkopp, Vaccaro and Carroll, 2002;
278 Miyazaki *et al.*, 2014; Zhang *et al.*, 2017; Zhang, Mazo-Vargas and Reed, 2017), as well as
279 behaviour, sex-specific phenotypes and reproductive maturation (Wilson *et al.*, 1976). These
280 genes share a common origin with the major royal jelly protein (MRJP) genes (Drapeau *et*
281 *al.*, 2006) which are crucial in caste development in honeybees. Like the MRJP genes, *yellow*
282 genes in honeybees have diverse spatial and temporal expression patterns. As our focus in *A.*
283 *plantaginis* has been on wing tissue, we are missing expression of genes in other tissues that
284 could be linked to other traits. Thus, it is not impossible to imagine that a *yellow* gene could
285 have a similar function to a MRJP in regulating the development of a complex phenotype.
286 Recent work with *Bicyclus anynana* showed that *yellow* functions as a repressor of male
287 courtship (Connahs *et al.*, 2022). On the other hand, sex specific behavioural phenotypes of
288 *yellow* mutants in *Drosophila* were found to be due to pigmentation effects (Massey *et al.*,
289 2019), so more evidence is needed to suggest a functional role for *yellow* genes outside of
290 pigmentation.

291 The duplication of *yellow-e* and surrounding regions in the white morphs suggests that the
292 yellow morph is the ancestral form. *Valkea* could have evolved in a stepwise fashion, first as

293 a tandem duplication then with a stop codon mutation altering the gene structure. Gene
294 duplications can facilitate adaptation and, in some examples, lead to polymorphism. Although
295 both *valkea* and *yellow-e* are overexpressed in the white morph, the topology weighting
296 suggests that *yellow-e* is not closely associated with the colour change. *Valkea* likely
297 represents an example of neofunctionalization, where the duplicated gene gains a different
298 function to the original gene copy.

299 Contrary to previous work that attributed red and yellow colours to pterins in another tiger
300 moth species (Gawne and Nijhout, 2019), we found high levels of 4-AHPEA in the yellow
301 wings confirming the presence of pheomelanins. These pigments have been widely associated
302 with red and yellow colours in mammals (e.g. Mcgraw and Wakamatsu, 2004), but only
303 relatively recently described in insects and likely to be more widespread than previously
304 thought. Yellow colours can also be produced by NBAD sclerotins which are sclerotizing
305 precursor molecules made from dopamine and these have an important role in the
306 sclerotization pathway for hardening the insect cuticle (Andersen, 2007; Barek, Evans and
307 Sugumaran, 2017) before becoming involved in melanisation (Barek *et al.*, 2018). Thus, we
308 suggest that the yellow colour arises partly from the NBAD sclerotins and partly from the
309 presence of pheomelanin pigments, which has been proposed in other Lepidoptera (Matsuoka
310 and Monteiro, 2018). While some 4-AHPEA also occurred in white wings, this may be due to
311 its role in production of cross-linking cuticular proteins and chitin during sclerotization
312 (Sugumaran, 2010). Upregulation of genes on the white allele could be acting as a repressor
313 of the generation of yellow colour. We suspect that *yellow* family genes play multiple roles
314 within the melanin production pathway. In the wood tiger moth, *yellow* affects the conversion
315 of DOPA into black dopamine melanin (Galarza, 2021). *Yellow-e* in particular has been
316 linked to larval colouration in *Bombyx mori* (Ito *et al.*, 2010) and adult colour in beetles
317 (Wang *et al.*, 2022), while another gene, *yellow-f*, has a role in eumelanin production (Barek
318 *et al.*, 2018).

319 In summary, we identified a structural variant containing a previously undescribed gene,
320 *valkea,* which is only present in white morphs of *A. plantaginis*. While functional studies are
321 needed to determine the exact function of this locus, the presence of a regulatory element
322 controlling wing colour and other traits via multiple downstream effects could explain how
323 multiple traits are linked to wing colouration. This complex polymorphism allows multiple
324 beneficial phenotypes to be inherited together, whereas recombination would separate

325 multiple loci leading to maladapted individuals. Our results provide the basis for further
326 exploration of the genetic basis of covarying behavioural and life-history traits, and offer an
327 intriguing example of how complex polymorphisms are maintained.

328 **Methods**

329 *Sampling*

330 Homozygous lines of white (WW) and yellow (yy) *Arctia plantaginis* moths were created
331 from Finnish populations at the University of Jyväskylä, Finland. Larvae were fed with wild
332 dandelion (*Taraxacum sp*.) and reared under natural light conditions, with an average day
333 temperature of 25ºC and night temperature between 15-20ºC. For the crosses, a heterozygous
334 male, created from crossing a heterozygous male with a homozygous yy female, was
335 backcrossed with a yy female. This was repeated to obtain four families totalling 172
336 offspring and 8 parents (Table S3). Samples from wild populations were caught in Southern
337 Finland (n=10) and Central Finland (n=20), where male morphs are either white or yellow,
338 Estonia (n=4), where males are mostly white, and Scotland (n=4), where males are yellow
339 (Table S4). In addition, we included 8 samples which are F1 offspring of wild Scottish
340 samples. Forty pupae with known genotypes from lab populations (20 WW and 20 yy) were
341 used for the RNA extractions.

342 *DNA extraction and sequencing*

343 For the lab crosses, DNA was extracted from two legs crushed with sterilised PVC pestles
344 using a Qiagen DNeasy Blood & Tissue kit, following the manufacturer's instructions.
345 Library preparation and GBS sequencing were performed by BGI Genomics on an Illumina
346 HiSeq X Ten. For the wild samples, DNA was extracted from the thoraces also with a Qiagen
347 kit. Library preparation and sequencing were performed by Novogene (Hong Kong, China).
348 150bp paired-end reads were sequenced on an Illumina NovaSeq 6000 platform.

349 *Linkage mapping analysis*

350 FASTQ reads were mapped using bowtie v2.3.2 (Langmead and Salzberg, 2012) to the
351 yellow *Arctia plantaginis* scaffold-level genome assembly (Yen *et al.*, 2020). BAM files
352 were sorted and indexed using SAMtools v.1.9 (Li *et al.*, 2009) and duplicates removed using
353 PicardTools MarkDuplicates (broadinstitute.github.io/picard). Twelve samples which had

354 aligned <30% were removed. Reads of the remaining samples had an average alignment of
355 94%. SNPs were called using SAMtools mpileup with minimum mapping quality set to 20
356 and bcftools call function. Lep-MAP3 (Rastas, 2017) was used for linkage map construction
357 and we ran the following modules: ParentCall2 which called 105,622 markers, Filtering2,
358 SeparateChromosomes2 with lodLimit=5 and sizeLimit=100, JoinSingles2All and
359 OrderMarkers2 with recombination2=0 to denote the lack of female recombination.
360 Genotypes were phased using the map2genotypes.awk script included with Lep-MAP3.
361 Markers were named based on the genomic positions of the SNPs in the reference genome
362 and the map.awk script, and this was used to further order the markers within the linkage
363 groups. This resolved 30 linkage groups. Although we expect that there are 31 chromosomes
364 in the moth genome, we suspect that the sex chromosome is missing in this assembly as the
365 yy individual used in the genome assembly was female (Yen *et al.*, 2020). A small number of
366 markers which caused long gaps at the beginning or end of linkage groups were manually
367 removed, leaving the final map 948.7cM long with 19,803 markers. Markers were well
368 distributed so we began the first analyses with this map. A linkage map was also assembled
369 using sequences aligned to the white reference and this separated into 31 linkage groups.

370 The QTL analysis was carried out in R/qtl (Broman *et al.*, 2003). Genotype probabilities were
371 calculated before running a genome scan using the *scanone* function with the Haley-Knott
372 method and binary model parameters, and including family as an additive covariate. The
373 phenotype was labelled as either 0 (Wy) or 1 (yy). We ran 5000 permutations to determine
374 the significance level for the QTL LOD scores. The *bayesint* function calculated the 95%
375 Bayesian confidence intervals around the significant marker.

376 *Analysis of whole genome sequences*

377 FASTQ reads were mapped to the yellow *A. plantaginis* genome assembly (Yen *et al.*, 2020)
378 using BWA-MEM v7.17 (Li, 2013). As before, BAM files were sorted and indexed, and
379 duplicates were removed. Genotyping and variant calling was carried out with the Genome
380 Analysis Toolkit (GATK) (McKenna *et al.*, 2010). Variants were called using
381 HaplotypeCaller (v.3.7) in GVCF mode, then gVCFs combined with GenomicsDBImport
382 (v.4.0). Joint genotyping was run with GenotypeGVCFs, set with a heterozygosity of 0.01,
383 and SNPs were called using SelectVariants. Finally, the set of 20,787,772 raw SNPs were
384 filtered using VariantFiltration and thresholds: quality by depth (QD > 2.0), root mean square
385 mapping quality (MQ > 50.0), mapping quality rank sum test (MQRankSum > −12.5), read

386 position rank sum test (ReadPosRankSum > −8.0), Fisher strand bias (FS < 60.0), and strand
387 odds ratio (SOR < 3.0). A set of 5,227,288 SNPs passed the filtering.

388 We carried out a Genome Wide Association Study (GWAS) using the R package GenABEL
389 v.1.8 (Aulchenko *et al.*, 2007). The set of filtered SNPs were converted to BED format with
390 PLINK2, keeping only biallelic SNPs (cog-genomics.org/plink/2.0/). Sites which were not in
391 Hardy-Weinberg equilibrium (p<0.01), or had a call rate of <0.5, were excluded. Following
392 this, 381,266 sites were retained across 40 individuals (out of 57). To account for population
393 stratification, we performed multidimensional scaling on kinship and identity-by-state (IBS)
394 information estimated from the data, and included this as a covariate in the association test.
395 Significance levels were calculated using Bonferroni corrected thresholds to account for
396 multiple testing. Central and Southern Finnish populations were pooled for this analysis,
397 based on a previous principal component analysis of these samples (Yen *et al.*, 2020).

398 In Yen et al. (2020), many of these samples were processed in the same way but aligned to
399 the white genome assembly (based on a white individual). We used the VCF file from this
400 study for a Twisst analysis (Martin and Van Belleghem, 2017) which included samples from
401 the Finnish, Estonian and Scottish populations. A minor allele frequency of 3 was applied to
402 the VCF with VCFtools, and this was phased using Beagle v5.1 (Browning, Zhou and
403 Browning, 2018). We generated neighbour joining trees with a window size of 50 using
404 PhyML and ran Twisst using scripts from github.com/simonhmartin/twisst. Read depth of the
405 W-mapped samples was calculated in 1kb windows across the candidate region using
406 BEDtools (v.2.20.1) multicov (Quinlan and Hall, 2010).

407 For analysis of structural variants, sequences from the white and yellow genome assemblies
408 were aligned using MAFFT v7.450 (Katoh and Standley, 2013) and viewed with Geneious.
409 Our focal sequence, scaffold 419 in the white genome, is the reverse complement of scaffold
410 206 in the yellow genome.

411 *Identification of candidate genes and tree construction*

412 To identify candidate genes in the QTL interval and GWAS region, we ran a protein
413 BLASTP v.2.4.0 search to identify *Heliconius melpomene* (Hmel2.5) proteins homologous to
414 predicted *A. plantaginis* proteins in the region from the genome annotation. Informative gene
415 names were obtained by performing a BLASTP search with the *H. melpomene* proteins
416 against all *Drosophila melanogaster* proteins in FlyBase v.FB2020_01 (flybase.org/blast).

417 For the *yellow* gene tree, we used Lepbase (Challi *et al.*, 2016) to search for *yellow* genes in
418 *Bombyx mori* (ASM15162v1). We identified *yellow-e* in *H. melpomene* by searching for
419 major royal jelly proteins, then comparing protein sequences of these against *Drosophila*
420 proteins in Flybase. The sequence for *Dmel yellow-e* was downloaded from Flybase. To make
421 the tree, coding sequences of all genes were aligned in Geneious using MAFFT v7.450
422 (Katoh and Standley, 2013), then the tree was constructed with PhyML using 10 bootstraps
423 (Guindon *et al.*, 2010).

424 *Differential gene expression*

425 We dissected the wings out of the pupae in Cambridge, UK. Pupae and larvae were sent to
426 Cambridge from Jyväskylä and were kept between 22 and 30˚C. Pupae were sexed and only
427 males were used. Dissections were made at 4 different stages: 72 hours after pupation (72h),
428 5 days after pupation (5d; counting 0-24 first hours after pupation as day 1), pre melanin
429 deposition (Pre-mel) and post melanin deposition (Mel). We sampled 5 individuals per stage
430 and genotype. Hindwings and forewings were stored separately in RNA-later (Sigma-
431 Aldrich) at 4 ˚C for 2 weeks and later transferred to -20 ˚C, while the rest of the body was
432 stored in pure ethanol.

433 Total RNA was extracted from hindwing tissue using a standard hybrid protocol. First, we
434 transferred the wing tissue into Trizol Reagent (Invitrogen) and homogenised it using dounce
435 tissue grinders (Sigma-Aldrich). Then, we performed a chloroform phase extraction, followed
436 by DNase treatment (Ambion) for 30 mins at 37˚C. We measured the concentration of total
437 RNA using Qubit Fluorometric Quantitation (Thermofisher) and performed a quality check
438 using an Agilent 4200 TapeStation (Agilent). The extracted total RNA was stored at -20˚C
439 before being sent to Novogene UK for sequencing.

440 We performed quality control and low-quality base and adapter trimming of the sequence
441 data using *TrimGalore!* We then mapped the trimmed reads to the two *A. plantaginis*
442 genomes using STAR. We performed a second round of mapping (2pass) including as input
443 the output splice junctions from the first round. The *A. plantaginis* genome annotations WW
444 and YY were included in each round of mapping respectively. We then used *FeatureCounts*
445 to count the mapped reads. Finally, we used DESeq2 to analyse the counts and perform the
446 DE analysis.

447 To identify the gene or genes controlling the development of wing colour in *A. plantaginis*,
448 we performed a genome wide differential expression analysis using limma-voom (Ritchie *et*
449 *al.*, 2015). First, we defined a categorical variable, 'GenStage', with 8 levels containing the
450 genotype and stage information of every individual sample (e.g. YY72h, WW72h, YY5days,
451 etc.). Then, we built the design matrix fitting a model with GenStage as the only fixed effect
452 factor contributing to the variance in gene expression and included family as a random effect
453 factor (gene expression ~ 0 + GenStage + (1|Family)). We then filtered lowly expressed
454 genes, which resulted in a reduction of the number of tested genes from 17,615 to 11,330
455 genes in the Y-mapped analysis and 17,930 to 10,920 in the W-mapped one. Finally, the list
456 of genes that are differentially expressed in each stage were extracted using the Benjamini-
457 Hochberg procedure to correct for multiple testing.

458 *Orthology assignment*

459 To infer genome wide orthology between *A. plantaginis* and *D. melanogaster*, we used
460 OrthoFinder (v2.5.4) (Emms and Kelly, 2019). We used proteomes from 6 Lepidoptera
461 species, *Plutela xylostella* (GCA_905116875_2)*, Bombyx mori* (GCF_014905235_1)*,*
462 *Spodoptera frugiperda* (GCF_011064685_1)*, Parnassius apollo* (GCA_907164705_1)*,*
463 *Pieris macdunnoughi* (GCA_905332375_1) *amd Pararge aegeria* (GCF_905163445_1) and
464 *Drosophila melanogaster* (GCF_000001215_4). We ran the primary_transcript.py utility
465 from OrthoFinder to extract only one transcript per protein, and then ran OrthoFinder with
466 default settings.

467 *Pigment analysis*

468 Solubility and fluorescence tests

469 Five hindwings from each morph were placed in two separate solvents (0.1M NaOH and 90%
470 MeOH) and left overnight. The supernatant was analysed with an Agilent Cary 8454 UV-
471 Visible spectrophotometer and the spectra compared to known spectra for various pigments.
472 A UV lamp (Philips TL8W/08 F8T5/BLB) used to test for fluorescence on the wings. The
473 presence of carotenoids was tested by placing wings into 1ml of pyridine and leaving at 95°C
474 for 4 hours (McGraw *et al.*, 2002). To these we added 1ml of 1:1 hexane:tert-butyl methyl
475 ether and 2ml of water before shaking and leaving overnight. Again, the supernatant was
476 measured with the spectrometer.

477 High-Performance Liquid Chromatography (HPLC) to test to eumelanin and ommochrome
478 pigments

479 To determine the type of melanin producing the black colour on the wings, we cut out
480 approximately 5mg of the black sections of the wings, from both females and males.
481 Eumelanin analysis was carried out according to (Borges *et al.*, 2001). Each sample was
482 added to a tube containing 820µl 0.5 M NaOH, 80µl 3% H_2O_2 and an internal standard
483 (48nmol phthalic acid) and heated in a boiling water bath for 20 minutes. Once cool, 20µl of
484 10% Na_2SO_3 and 250µl of 6M HCl was added. Samples were then extracted twice with 7ml
485 of ethyl acetate. Ethyl acetate was dried at 45 °C under a stream of nitrogen. The residue was
486 dissolved into 0.5ml of 0.1% formic acid.

487 We carried out high-performance liquid chromatography on an Agilent 1100 HPLC. 20µl of
488 the sample was injected into a Waters Atlantis T3, 100 x 3.0mm i.d. analytical column
489 (Waters, Milford, MA, USA). The column was set to 25°C and analytes were detected at
490 wavelength 280nm. The HPLC mobile phase consisted of two eluents: UHQ-water/MeOH
491 (98/2; v/v) with 0.1% formic acid and UHQ-water/MeOH (40/60; v/v) with 0.1% formic acid.
492 Flow rate was 0.4 ml/min and the used gradient started with 100% of eluent A and ramped
493 evenly from time 0 to 15 minutes to 40:60 (A:B; v/v), held at 40:60 for 6 minutes and ramped
494 evenly back to initial eluent composition (100% A) over 5 minutes. We compared
495 chromatograms obtained from the samples to the chromatograms obtained from synthetic
496 melanin, ink from sepia officinalis and black human hair.

497 HPLC was also applied to observe the possible presence of ommochrome pigments. Injection
498 volume was 10µl and for the separation we used the same Waters Atlantis T3 column (100 x
499 3.0 mm i.d.) set to 30°C. Solvent A was UHQ-water and B was acetonitrile (ACN), both
500 containing 0.1% formic acid. Flow rate was 0.4ml/min and the used gradient was as follows:
501 Initial flow ratio was 98/2 water/ACN (v/v) ramping then evenly from time 1 to 15 min to
502 30:70 water:ACN (v/v), held for 1.5 min and then ramped evenly back to initial eluent
503 composition over 0.5 minutes. The column was stabilised for 7 minutes before a new run.

504 Pheomelanin analysis

505 Samples were analysed for pheomelanin content according to the method of Kolb *et al.*
506 (1997) with modifications. A 2mg sample was placed in a screw-capped tube with 100µl
507 water, 500µl ~55-58% hydrogen iodide (HI), and 20µl 50% hypophosphorous acid (H_3PO_2).

508 Samples were capped tightly and hydrolysed for 20 hours at 130°. After cooling, samples
509 were evaporated under nitrogen flow, then dissolved in 1ml of 0.1M HCl and purified with
510 solid phase extraction. Strata SCX cartridges were preconditioned with 2ml of methanol, 3ml
511 of water and 1ml of 0.1M HCl. Sample was then applied to the cartridge, washed with 1ml of
512 0.1M HCl, and finally eluted with 1ml of methanol (MeOH): 0.5M ammonium acetate
513 ($NH_4CH_3CO_2$) (20:80 v/v).

514 Hydrogen Iodide hydrolysis products were determined by a Dionex high-performance liquid
515 chromatograph equipped with pulsed amperometric detection (HPLC/PAD). A Phenomenex
516 Kinetex C18 column (150 x 4.6 mm i.d.; 5µm particle size) with a gradient elution (Table S5)
517 at a flow rate of 0.9 ml min^{-1} with the eluents: (A) sodium citrate buffer (Hines *et al.*, 2017)
518 in ultra-high-quality water (internal resistance ≥ 18.2 MΩ cm; Milli-Q Plus; Millipore,
519 Bedford, MA, USA) and (B) methanol were used for the separation. Dionex ED-50 pulsed
520 amperometric detector (Dionex, Sunnyvale, CA, USA) equipped with a disposable working
521 electrode by using a Dionex waveform A with potentials presented in Table S6 was used for
522 detection. 4-AHP, 3-AHPEA and 4-AHPEA standards used in calibration were kindly offered
523 from the laboratory of Emeritus Professor Wakamatsu and the preparation method is
524 described in (Wakamatsu *et al.*, 2014).

525 **Acknowledgements**

526 We thank Kaisa Suisto and the greenhouse staff for insect rearing, and Elisa Salmivirta and
527 Sari Viinikainen for lab assistance. Thanks to Emeritus Prof. Shosuke Ito for providing
528 pheomelanin standards and to Bodo Wilts for advice on the pigment analyses.

529 This work was supported by Academy of Finland grants to MB (#343356) and JM (projects
530 345091 and 328474).

531 **Data availability**

532 All the scripts used for mapping and DE analysis will be uploaded to an online repository.
533 Scripts and data for the QTL and GWAS analyses can currently be found at
534 github.com/mnbrien/Aplantaginis-male-colour. Raw sequencing data of wild samples has
535 previously been deposited in ENA, study accession No. PRJEB36595.

536

537 **References**

538 Andersen, S. O. (2007) 'Involvement of tyrosine residues, N-terminal amino acids, and β-
539 alanine in insect cuticular sclerotization', *Insect Biochemistry and Molecular Biology*, 37(9),
540 pp. 969–974. doi: https://doi.org/10.1016/j.ibmb.2007.05.002.

541 Andrade, P. *et al.* (2019) 'Regulatory changes in pterin and carotenoid genes underlie
542 balanced color polymorphisms in the wall lizard', *Proceedings of the National Academy of*
543 *Sciences of the United States of America*, 116(12), pp. 5633–5642. doi:
544 10.1073/pnas.1820320116.

545 Aulchenko, Y. S. *et al.* (2007) 'GenABEL: an R library for genome-wide association
546 analysis', *Bioinformatics*, 23(10), pp. 1294–1296. doi: 10.1093/bioinformatics/btm108.

547 Barek, H. *et al.* (2018) 'Insect cuticular melanins are distinctly different from those of
548 mammalian epidermal melanins', *Pigment Cell and Melanoma Research*, 31(3), pp. 384–392.
549 doi: 10.1111/pcmr.12672.

550 Barek, H., Evans, J. and Sugumaran, M. (2017) 'Unraveling complex molecular
551 transformations of N-β-alanyldopamine that account for brown coloration of insect cuticle',
552 *Rapid Communications in Mass Spectrometry*, 31(16), pp. 1363–1373. doi:
553 https://doi.org/10.1002/rcm.7914.

554 Borges, C. R. *et al.* (2001) 'Relationship of Melanin Degradation Products to Actual Melanin
555 Content: Application to Human Hair', *Analytical Biochemistry*, 290(1), pp. 116–125. doi:
556 https://doi.org/10.1006/abio.2000.4976.

557 Briolat, E. S. *et al.* (2019) 'Diversity in warning coloration: selective paradox or the norm?',
558 *Biological Reviews*, 94(2), pp. 388–414. doi: 10.1111/brv.12460.

559 Broman, K. W. *et al.* (2003) 'R/qtl: QTL mapping in experimental crosses', *Bioinformatics*,
560 19(7), pp. 889–890. doi: 10.1093/bioinformatics/btg112.

561 Browning, B. L., Zhou, Y. and Browning, S. R. (2018) 'A One-Penny Imputed Genome from
562 Next-Generation Reference Panels', *The American Journal of Human Genetics*, 103(3), pp.
563 338–348. doi: https://doi.org/10.1016/j.ajhg.2018.07.015.

564 Challi, R. J. *et al.* (2016) 'Lepbase: the Lepidopteran genome database', *bioRxiv*, p. 56994.
565 doi: 10.1101/056994.

566 Connahs, H. *et al.* (2022) 'The yellow gene regulates behavioural plasticity by repressing
567 male courtship in Bicyclus anynana butterflies', *Proceedings of the Royal Society B:*
568 *Biological Sciences*, 289(1972), p. 20212665. doi: 10.1098/rspb.2021.2665.

569 Cott, H. B. (1940) *Adaptive coloration in animals*. London: Methuen.

570 Cuthill, I. C. *et al.* (2017) 'The biology of color', *Science*, 357(6350). doi:
571 10.1126/science.aan0221.

572 Drapeau, M. D. *et al.* (2006) 'Evolution of the Yellow/Major Royal Jelly Protein family and
573 the emergence of social behavior in honey bees', *Genome Research*, 16(11), pp. 1385–1394.

574 doi: 10.1101/gr.5012006.

575 Emms, D. M. and Kelly, S. (2019) 'OrthoFinder: phylogenetic orthology inference for
576 comparative genomics', *Genome Biology*, 20(1), p. 238. doi: 10.1186/s13059-019-1832-y.

577 Endler, J. A. (1988) 'Frequency-dependent predation, crypsis and aposematic coloration',
578 *Philosophical Transactions of the Royal Society B: Biological Sciences*, 319, pp. 505–523.

579 Ferguson, L. C. *et al.* (2011) 'Evolution of the insect yellow gene family', *Molecular Biology*
580 *and Evolution*, 28(1), pp. 257–272. doi: 10.1093/molbev/msq192.

581 Funk, E. R. *et al.* (2021) 'A supergene underlies linked variation in color and morphology in
582 a Holarctic songbird', *Nature Communications*, 12(1), p. 6833. doi: 10.1038/s41467-021-
583 27173-z.

584 Galarza, J. A. *et al.* (2014) 'Temporal relationship between genetic and warning signal
585 variation in the aposematic wood tiger moth (Parasemia plantaginis)', *Molecular Ecology*,
586 23(20), pp. 4939–4957. doi: 10.1111/mec.12913.

587 Galarza, J. A. (2021) 'Comparative transcriptomics of albino and warningly-coloured
588 caterpillars', *Ecology and Evolution*, 11(12), pp. 7507–7517. doi:
589 https://doi.org/10.1002/ece3.7581.

590 Galván, I. *et al.* (2015) 'Insects synthesize pheomelanin', *Pigment Cell and Melanoma*
591 *Research*, 28(5), pp. 599–602. doi: 10.1111/pcmr.12397.

592 Gawne, R. and Nijhout, H. F. (2019) 'Expanding the nymphalid groundplan's domain of
593 applicability: pattern homologies in an arctiid moth (Utetheisa ornatrix)', *Biological Journal*
594 *of the Linnean Society*, 126(4), pp. 912–924. doi: 10.1093/biolinnean/bly193.

595 Gordon, S. P. *et al.* (2015) 'Colour polymorphism torn apart by opposing positive frequency-
596 dependent selection, yet maintained in space', *Journal of Animal Ecology*, 84(6), pp. 1555–
597 1564. doi: 10.1111/1365-2656.12416.

598 Guindon, S. *et al.* (2010) 'New Algorithms and Methods to Estimate Maximum-Likelihood
599 Phylogenies: Assessing the Performance of PhyML 3.0', *Systematic Biology*, 59(3), pp. 307–
600 321. doi: 10.1093/sysbio/syq010.

601 Hegna, R. H., Galarza, J. A. and Mappes, J. (2015) 'Global phylogeography and geographical
602 variation in warning coloration of the wood tiger moth (Parasemia plantaginis)', *Journal of*
603 *Biogeography*, 42(8), pp. 1469–1481. doi: 10.1111/jbi.12513.

604 Hines, H. M. *et al.* (2017) 'Melanic variation underlies aposematic color variation in two
605 hymenopteran mimicry systems', *PLoS ONE*, 12(7), pp. 1–17. doi:
606 10.1371/journal.pone.0182135.

607 Huu, C. N. *et al.* (2020) 'Supergene evolution via stepwise duplications and
608 neofunctionalization of a floral-organ identity gene', *Proceedings of the National Academy of*
609 *Sciences of the United States of America*, 117(37), pp. 23148–23157. doi:
610 10.1073/pnas.2006296117.

611 Huxley, J. (1955) 'Morphism and evolution', *Heredity*, 9(1), pp. 1–52. doi:

612 10.1038/hdy.1955.1.

613 Ito, K. *et al.* (2010) 'Yellow-e determines the color pattern of larval head and tail spots of the
614 silkworm Bombyx mori', *Journal of Biological Chemistry*, 285(8), pp. 5624–5629. doi:
615 10.1074/jbc.M109.035741.

616 Jorge García, A., Polidori, C. and Nieves-Aldrey, J. L. (2016) 'Pheomelanin in the secondary
617 sexual characters of male parasitoid wasps (Hymenoptera: Pteromalidae)', *Arthropod*
618 *Structure & Development*, 45(4), pp. 311–319. doi: https://doi.org/10.1016/j.asd.2016.05.001.

619 Joron, M. *et al.* (2006) 'A Conserved Supergene Locus Controls Colour Pattern Diversity in
620 *Heliconius* Butterflies', *PLoS Biology*, 4(10), pp. 1831–1840. doi:
621 10.1371/journal.pbio.0040303.

622 Katoh, K. and Standley, D. M. (2013) 'MAFFT Multiple Sequence Alignment Software
623 Version 7: Improvements in Performance and Usability', *Molecular Biology and Evolution*,
624 30(4), pp. 772–780. doi: 10.1093/molbev/mst010.

625 Kayser, H. (1985) 'Pigments', in Kerkut, G. A. and Gilbert, L. I. (eds) *Comparative Insect*
626 *Physiology, Biochemistry, and Pharmacology*. Oxford: Pergamon Press, pp. 367–415.

627 Kolb, A. M. *et al.* (1997) 'Determination of Pheomelanin by Measurement of
628 Aminohydroxyphenylalanine Isomers with High-Performance Liquid Chromatography',
629 *Analytical Biochemistry*, 252(2), pp. 293–298. doi: https://doi.org/10.1006/abio.1997.2342.

630 Kratochwil, C. *et al.* (2018) 'Agouti-related peptide 2 facilitates convergent evolution of
631 stripe patterns across cichlid fish radiations', *Science*, 362(6413), pp. 457–460. doi:
632 10.1126/science.aao6809.

633 Kunte, K. *et al.* (2014) 'doublesex is a mimicry supergene', *Nature*, 507(7491), pp. 229–232.
634 doi: 10.1038/nature13112.

635 Küpper, C. *et al.* (2016) 'A supergene determines highly divergent male reproductive morphs
636 in the ruff', *Nature Genetics*, 48(1), pp. 79–83. doi: 10.1038/ng.3443.

637 Langmead, B. and Salzberg, S. L. (2012) 'Fast gapped-read alignment with Bowtie 2',
638 *Nature Methods*, 9, p. 357. Available at: http://dx.doi.org/10.1038/nmeth.1923.

639 Li, H. *et al.* (2009) 'The Sequence Alignment/Map format and SAMtools', *Bioinformatics*,
640 25(16), pp. 2078–2079. doi: 10.1093/bioinformatics/btp352.

641 Li, H. (2013) 'Aligning sequence reads, clone sequences and assembly contigs with BWA-
642 MEM', *arXiv*, p. 1303.3997.

643 Linnen, C. R. *et al.* (2013) 'Adaptive Evolution of Multiple Traits Through Multiple
644 Mutations at a Single Gene', *Science*, 339(6125), pp. 1312–1316. doi:
645 10.1126/science.1233213.

646 Lowry, D. B. and Willis, J. H. (2010) 'A Widespread Chromosomal Inversion Polymorphism
647 Contributes to a Major Life-History Transition, Local Adaptation, and Reproductive
648 Isolation', *PLOS Biology*, 8(9), p. e1000500. Available at:
649 https://doi.org/10.1371/journal.pbio.1000500.

650 Martin, S. H. and Van Belleghem, S. M. (2017) 'Exploring Evolutionary Relationships
651 Across the Genome Using Topology Weighting', *Genetics*, 206(1), pp. 429 LP – 438. doi:
652 10.1534/genetics.116.194720.

653 Massey, J. H. *et al.* (2019) 'The yellow gene influences Drosophila male mating success
654 through sex comb melanization', *eLife*. Edited by K. VijayRaghavan and C. L. Peichel, 8, p.
655 e49388. doi: 10.7554/eLife.49388.

656 Matsuoka, Y. and Monteiro, A. (2018) 'Melanin Pathway Genes Regulate Color and
657 Morphology of Butterfly Wing Scales', *Cell Reports*, 24(1), pp. 56–65. doi:
658 10.1016/j.celrep.2018.05.092.

659 McGraw, K. J. *et al.* (2002) 'The effect of dietary carotenoid access on sexual dichromatism
660 and plumage pigment composition in the American goldfinch', *Comparative Biochemistry*
661 *and Physiology Part B: Biochemistry and Molecular Biology*, 131(2), pp. 261–269. doi:
662 https://doi.org/10.1016/S1096-4959(01)00500-0.

663 Mcgraw, K. J. and Wakamatsu, K. (2004) 'Melanin Basis of Ornamental Feather Colors in
664 Male Zebra Finches', *The Condor*, 106(3), pp. 686–690. doi: 10.1093/condor/106.3.686.

665 McKenna, A. *et al.* (2010) 'The Genome Analysis Toolkit: A MapReduce framework for
666 analyzing next-generation DNA sequencing data', *Genome Research*, 20, pp. 1297–1303.
667 doi: 10.1101/gr.107524.110.

668 McKinnon, J. S. and Pierotti, M. E. R. (2010) 'Colour polymorphism and correlated
669 characters: Genetic mechanisms and evolution', *Molecular Ecology*, 19(23), pp. 5101–5125.
670 doi: 10.1111/j.1365-294X.2010.04846.x.

671 Miyazaki, S. *et al.* (2014) 'Sexually Dimorphic Body Color Is Regulated by Sex-Specific
672 Expression of Yellow Gene in Ponerine Ant, Diacamma Sp', *PLOS ONE*, 9(3), p. e92875.
673 Available at: https://doi.org/10.1371/journal.pone.0092875.

674 Nadeau, N. J. *et al.* (2016) 'The gene *cortex* controls mimicry and crypsis in butterflies and
675 moths', *Nature*, 534(7605), pp. 106–110. doi: 10.1038/nature17961.

676 Nishikawa, H. *et al.* (2015) 'A genetic mechanism for female-limited Batesian mimicry in
677 Papilio butterfly', *Nature Genetics*, 47(4), pp. 405–409. doi: 10.1038/ng.3241.

678 Nokelainen, O. *et al.* (2012) 'Trade-off between warning signal efficacy and mating success
679 in the wood tiger moth', *Proceedings of the Royal Society B: Biological Sciences*, 279(1727),
680 pp. 257–265. doi: 10.1098/rspb.2011.0880.

681 Nokelainen, O. *et al.* (2014) 'Changes in predator community structure shifts the efficacy of
682 two warning signals in Arctiid moths', *Journal of Animal Ecology*, 83(3), pp. 598–605. doi:
683 10.1111/1365-2656.12169.

684 Nokelainen, O. *et al.* (2022) 'Genetic colour variation visible for predators and conspecifics
685 is concealed from humans in a polymorphic moth', *Journal of Evolutionary Biology*,
686 (February), pp. 467–478. doi: 10.1111/jeb.13994.

687 Orteu, A. and Jiggins, C. D. (2020) 'The genomics of coloration provides insights into
688 adaptive evolution', *Nature Reviews Genetics*, 21(8), pp. 461–475. doi: 10.1038/s41576-020-

0234-z.

Polidori, C., Jorge, A. and Ornosa, C. (2017) 'Eumelanin and pheomelanin are predominant pigments in bumblebee (Apidae: Bombus) pubescence', *PeerJ*, 2017(5), pp. 1–21. doi: 10.7717/peerj.3300.

Quinlan, A. R. and Hall, I. M. (2010) 'BEDTools: a flexible suite of utilities for comparing genomic features', *Bioinformatics*, 26(6), pp. 841–842. doi: 10.1093/bioinformatics/btq033.

Rastas, P. (2017) 'Lep-MAP3: robust linkage mapping even for low-coverage whole genome sequencing data', *Bioinformatics*, 33, pp. 3726–3732. doi: 10.1093/bioinformatics/btx494.

Reed, R. D. *et al.* (2011) '*optix* drives the repeated convergent evolution of butterfly wing pattern mimicry', *Science*, 333, pp. 1137–1141. doi: 10.1126/science.1208227.

Ritchie, M. E. *et al.* (2015) 'limma powers differential expression analyses for RNA-sequencing and microarray studies', *Nucleic Acids Research*, 43(7), pp. e47–e47. doi: 10.1093/nar/gkv007.

Rojas, B. *et al.* (2017) 'How to fight multiple enemies: Target-specific chemical defences in an aposematic moth', *Proceedings of the Royal Society B: Biological Sciences*, 284(1863). doi: 10.1098/rspb.2017.1424.

Rojas, B., Gordon, S. P. and Mappes, J. (2015) 'Frequency-dependent flight activity in the colour polymorphic wood tiger moth', *Current Zoology*, 61(4), pp. 765–772. doi: 10.1093/czoolo/61.4.765.

Rönkä, K. *et al.* (2020) 'Geographic mosaic of selection by avian predators on hindwing warning colour in a polymorphic aposematic moth', *Ecology Letters*, 23(11), pp. 1654–1663. doi: https://doi.org/10.1111/ele.13597.

Shamim, G. *et al.* (2014) 'Biochemistry and biosynthesis of insect pigments', *European Journal of Entomology*, 111(2), pp. 149–164. doi: 10.14411/eje.2014.021.

Sugumaran, M. (2010) 'Chapter 5 - Chemistry of Cuticular Sclerotization', in Simpson, S. J. B. T.-A. in I. P. (ed.). Academic Press, pp. 151–209. doi: https://doi.org/10.1016/B978-0-12-381387-9.00005-1.

Suomalainen, E. (1938) 'Die erblichkeitsverhältnisse des männlichen dimorphismus bei parasemia plantaginis', *Hereditas*, 24, pp. 386–390.

Thompson, M. J. and Jiggins, C. D. (2014) 'Supergenes and their role in evolution', *Heredity*, 113(1), pp. 1–8. doi: 10.1038/hdy.2014.20.

Timmermans, M. J. T. N. *et al.* (2014) 'Comparative genomics of the mimicry switch in Papilio dardanus', *Proceedings of the Royal Society B: Biological Sciences*, 281(1787). doi: 10.1098/rspb.2014.0465.

Tuttle, E. M. *et al.* (2016) 'Divergence and Functional Degradation of a Sex Chromosome-like Supergene', *Current Biology*, 26(3), pp. 344–350. doi: https://doi.org/10.1016/j.cub.2015.11.069.

Umebachi, Y. (1975) ‘Further studies on the dopamine derivative, SN-1 derived from the yellow pigments of Papilio xuthus’, *Insect Biochemistry*, 5, pp. 73–92.

Wakamatsu, K. *et al.* (2014) ‘Reduction of the Nitro Group to Amine by Hydroiodic Acid to Synthesize o-Aminophenol Derivatives as Putative Degradative Markers of Neuromelanin’, *Molecules* . doi: 10.3390/molecules19068039.

Wakamatsu, K., Ito, S. and Rees, J. L. (2002) ‘The Usefulness of 4-Amino-3-hydroxyphenylalanine as a Specific Marker of Pheomelanin’, *Pigment Cell Research*, 15(3), pp. 225–232. doi: https://doi.org/10.1034/j.1600-0749.2002.02009.x.

Wang, J. *et al.* (2013) ‘A Y-like social chromosome causes alternative colony organization in fire ants’, *Nature*, 493(7434), pp. 664–668. doi: 10.1038/nature11832.

Wang, P. *et al.* (2022) ‘Yellow-b, -c, -e and -h are required for normal body coloration in Henosepilachna vigintioctopunctata’, *Archives of Insect Biochemistry and Physiology*, 109(2), p. e21856. doi: https://doi.org/10.1002/arch.21856.

Wilson, R. *et al.* (1976) ‘Behavioural pleiotropy of the yellow gene in Drosophila melanogaster’, *Genetical Research*. 2009/04/14, 28(1), pp. 75–88. doi: DOI: 10.1017/S0016672300016748.

Wittkopp, P. J., Vaccaro, K. and Carroll, S. B. (2002) ‘Evolution of yellow gene regulation and pigmentation in Drosophila’, *Current Biology*, 12(18), pp. 1547–1556. doi: 10.1016/S0960-9822(02)01113-2.

Yen, E. C. *et al.* (2020) ‘A haplotype-resolved, de novo genome assembly for the wood tiger moth (Arctia plantaginis) through trio binning’, *GigaScience*, 9(8), pp. 1–12. doi: 10.1093/gigascience/giaa088.

Zhang, L. *et al.* (2017) ‘Genetic basis of melanin pigmentation in butterfly wings’, *Genetics*, 205(4), pp. 1537–1550. doi: 10.1534/genetics.116.196451.

Zhang, L., Mazo-Vargas, A. and Reed, R. D. (2017) ‘Single master regulatory gene coordinates the evolution and development of butterfly color and iridescence’, *Proceedings of the National Academy of Sciences*, 114, pp. 10707–10712. doi: 10.1073/pnas.1709058114.